Heterogeneity Impacts of Natural and Socioeconomic Factors and Their Interactions On $PM_{2.5}$ in the Yangtze River Economic Belt

Siyou Xia
Institute of Geographic Sciences and Natural Resources Research
Xiaojie Liu
School of Geographic and Oceanographic Sciences, Nanjing University
Qing Liu
School of Geography and Planning, Sun Yat-sen University
Yannan Zhou
Institute of Geographic Sciences and Natural Resources Research
Yu Yang (yangyu@igsnrr.ac.cn)
Institute of Geographic Sciences and Natural Resources Research

Research Article

Keywords: epidemic, spatiotemporal, socioeconomic, anthropogenic, pollution

Posted Date: October 21st, 2021

DOI: https://doi.org/10.21203/rs.3.rs-961854/v1

Abstract

Haze has reached epidemic levels in many cities of China in recent years. Only limited studies have explored the impacts of driving factors and their interactions on the spatiotemporal heterogeneity of $PM_{2.5}$. This paper investigates the spatiotemporal characteristics of $PM_{2.5}$ pollution through spatial analytical methods based on retrievals of satellite aerosol optical depth (AOD) data from the Yangtze River Economic Belt (YREB) between 2000 and 2017. Geographically weighted regression (GWR) and geodetector models were applied to assess the directions and strength of association between natural and socioeconomic conditions and $PM_{2.5}$ pollution. The results indicate that the annual concentration range of $PM_{2.5}$ in the YREB was 23.49–37.37 μg/m^3 with an initial increasing and later declining trend. The $PM_{2.5}$ pollution displays a diagonal spatial distribution pattern of high in northeast and low in southwest and a noticeable spatial convergence. The spatial variability of $PM_{2.5}$ pollution was enlarged and its main fractal dimension was in the northeast–southwest direction. There were clear spatiotemporal variations in the impact of natural and anthropogenic factors on $PM_{2.5}$ pollution. Interactive factors included bi-factor and nonlinear enhancements. Our findings contribute to a better understanding of the impact mechanisms of $PM_{2.5}$ pollution and the geographical factors in forming persistent and highly polluted areas and imply that more specific coping strategies need to be targeted in various areas toward successful particulate pollution prevention and control.

Introduction

Haze is present in most urban regions of the world and is a global environmental problem. Rapid increase in urbanization and industrialization of many cities in China has caused haze pollution, which is dominated by enhanced concentration of $PM_{2.5}$ (particulate matter with an aerodynamic diameter ≤ 2.5 μm). $PM_{2.5}$ has significant adverse impacts on public health, environment, and climate because of its small diameter, high activity, and ability to transport noxious substances in air with long residence times[1–3]. Epidemiological studies have confirmed that $PM_{2.5}$ can induce various respiratory and cardiovascular diseases, impair the body's immune system, and increase mortality of people exposed to it[4,5]. More than 1.3 million people in China die prematurely each year due to prolonged exposure to polluted air, which is about 40% of the global total[6]. The International Agency for Research on Cancer (IARC) classified $PM_{2.5}$ as a human carcinogen in 2013[7]. Moreover, continuous haze damages the overall image of a city and weakens the attraction of tourism, talent, and investments, which restrict sustainable development of the urban economy[8–10]. The issues related to cleaning the air have aroused attentions at domestic and board largely.

$PM_{2.5}$ has garnered significant attention of the atmospheric and climate science community and many studies have explored environmental issues related to it including on spatiotemporal distribution and driving factors. Research on spatial patterns of $PM_{2.5}$ mainly focus on environmental coping policies by identifying its distribution patterns and their spatial effects. These studies reveal that $PM_{2.5}$ pollution has

regional, cumulative, and compound effects and it possesses significant spatiotemporal variability[11–13]. Additionally, $PM_{2.5}$ pollution is not restricted to the local environment and it can be diffused or transferred to neighbouring areas largely through external forces such as atmospheric circulation causing spillover effects[14]. The identification and estimation of $PM_{2.5}$ pollution with spatial characteristics should be studied by means of spatial analytical methods rather than by traditional statistical theory based on independent observations[15]. Spatial statistics started in the 1970s with the goal of understanding spatial dependence, spatial association, and other relations among data related to geographical locations with wide applications in natural and social sciences. The accurate identification of $PM_{2.5}$ concentration drivers can provide a strong theoretical basis for the prevention and control of air pollution. Therefore, many scholars are committed to understand source analyses, emission inventories, chemical conversion, and regional transport of $PM_{2.5}$ and have achieved significant results. In general, $PM_{2.5}$ is considered to be emitted from local sources, including primary sources such as traffic fumes, industrial activities, soil dust, biomass, and coal combustion, and secondary sources of gaseous pollutants (such as SO_2, NOx, and NH_3) formed by complex chemical reactions, and sources from regional transmission [10,16–18]. Thus, a local $PM_{2.5}$ concentration change is the result of the combined action of natural conditions and anthropogenic factors[19–20]. Natural factors such as meteorological conditions, topography, and vegetation play important roles in the generation, accumulation, transfer, diffusion, and settlement of $PM_{2.5}$ and profoundly affect its local concentration[20–21]. With respect to the influence of socioeconomic factors related to anthropogenic activities on the distribution of $PM_{2.5}$, studies suggest that energy-intensive economic growth and non-ecological urbanization cause increase in $PM_{2.5}$ concentration implying that economic development, urbanization, industrialization, land use type, energy use mix and efficiency can affect urban air quality[13,22–24]. These studies provide many insights on urban particle pollution from the perspectives of anthropogenic and natural conditions.

The Yangtze River Economic Belt (YREB) is one of China's most crucial economic and ecological corridors that connects three national urban agglomerations of the Sichuan–Chongqing, the middle reaches of the Yangtze River, and the Yangtze River Delta (YRD). The YREB accounts for more than 40% of China's population and GDP, and its unique geographical advantages and vast economic hinterland make it the region with the greatest economic growth potential in the next 30 years[25]. However, urban air quality along the Yangtze has been deteriorating and it has suffered from varying degrees of haze pollution due to continuous and intense industrial and human activities[26]. Recently, some areas in the middle–lower reaches of the Yangtze have had more than 100 haze d yr^{-1}, with some cities even exceeding 200 d yr^{-1} [27]. In the Chengdu–Chongqing and Yunnan–Guizhou areas of the upper reaches, the environment is relatively vulnerable as economic development is being scaled up [28]. The alleviation of haze pollution involves the integrity of the ecological and environmental system and the quality of local people's life[9]. In 2014, the development of the YREB was given the status of a national strategy leading to the fact that potential conflicts between economic growth and environmental protection may be more prominent than ever before[29]. In 2018, President Xi emphasized on the protection of the ecological and environmental

status of the YREB. Hence, the ecological and environmental protection of the Yangtze is a priority for the government of China[25].

Until now, studies on the environmental problems of the YREB have mainly focused on the macrolevel, including environmental quality and risk assessment, low-carbon economy, and sustainable development strategy[9,28]. Studies on environmental problems at the microlevel focus more on water pollution, while studies on air pollution are still insufficient[27]. As the China National Environmental Monitoring Centre (CNEMC) did not include $PM_{2.5}$ in its monitoring index system until 2012, there were relatively few studies focusing on $PM_{2.5}$ in the YREB before that[30]. The CNEMC began widespread real-time monitoring of $PM_{2.5}$ since 2013. Furthermore, the use of remote sensing data for long-term time series research was limited to local areas and specific cities[31] and studies on influencing factors mostly were in terms of the overall perspective. Obvious spatial differences in the natural conditions and socioeconomic development of various regions exist, and hence, a global analysis cannot reveal the spatial heterogeneity of the effects of various factors [32]. On the other hand, majority researches did not conduct spatial analysis from a geographical view. Although some research has considered spatial dependence of $PM_{2.5}$ pollution, they still neglected spatial differentiation of $PM_{2.5}$ level at the urban agglomeration scale and lacked analysis of the interactive mechanism between factors, which may lead to incomplete and biased conclusions[33].

In this study, we attempt to fill the aforesaid gaps. We consider 130 cities within the YREB as the research area and employ geostatistical and spatial analytical methods to summarize the spatiotemporal evolutionary features of $PM_{2.5}$ pollution. Furthermore, we adopt geographically weighted regression (GWR) model and geographical detectors to quantitatively analyse spatial differentiation and interactive effects of socioeconomic and natural conditions on $PM_{2.5}$ during various periods. Thus, our study is significant in terms of meeting the demand for air quality improvements in the YREB and sheds light on implementing effective urban $PM_{2.5}$ pollution abatement policies.

Data And Methods

Study area. The YREB spans the eastern, central, and western regions of China, including nine provinces (Zhejiang, Jiangsu, Jiangxi, Anhui, Hubei, Hunan, Sichuan, Yunnan, and Guizhou) and two municipalities (Shanghai and Chongqing) (Fig. 1). The YREB comprises of an area of 2.05×10^6 km^2 accounting for 21.3% of the country's land area. Moreover, its economy and population density are 6.2 and 4.5 times the national average, respectively, establishing its incomparable role in China's development strategies[8]. However, the YREB is an ecologically vulnerable zone, and hence, assessing $PM_{2.5}$ pollution in the region is of great strategic significance for national ecological security and regional sustainable development[28].

Data acquisition and processing. Our data sources have four components. (1) $PM_{2.5}$ concentration data from satellite retrievals. The annual average concentration of $PM_{2.5}$ was obtained from the global surface

raster value of 0.01° × 0.01°, which was released by the Atmospheric Composition Analysis Group (ACAG) (http://fizz.phys.dal.ca). This $PM_{2.5}$ remote sensing inversion data set has the largest global coverage, the longest time span, and the highest accuracy, and it has been widely verified and effectively applied in China[34]. In order to verify the accuracy of the dataset in the YREB, we calculated the annual concentration of each station through real-time monitoring data of the YREB from 2015 to 2017 obtained from the CNEMC (http://www.cnemc.cn), and correlated it with the $PM_{2.5}$ concentration from the remote sensing inversion data at the corresponding position. The correlation coefficient was 0.82 and significant indicating a strong correlation and consistency between these data sets. (2) Data of natural parameters. The natural parameters include wind, precipitation, vegetation, and topography. The normalized differential vegetation index (NDVI) is the best indicator of vegetation coverage and growth status, and the original data was derived from the National Aeronautics and Space Administration (NASA) (http://modis.gsfc.nasa. gov), while the supporting data were obtained from the Resource and Environment Data Cloud Platform (http://www.resdc.cn). (3) Socioeconomic data. Socioeconomic data include per capita GDP, population density, economic density, urbanization rate, industrial structure, and energy consumption. Studies have shown that there is a significant linear correlation between night light data from Defense Meteorological Satellite Program/Operational Line Scanner (DMSP/OLS) and energy consumption[35]. We converted the light intensity to grey pixel values and used the sum of all DMSP/OLS raster grey values in each region as an indicator of energy consumption in the region. The DMSP/OLS dataset was obtained from the National Oceanic and Atmospheric Administration (NOAA) (https://www.ngdc.noaa.gov) and the remaining data were collected from the China Urban Statistics Yearbook published by the National Bureau of Statistics (http://www.stats.gov.cn/). (4) Geographic information data. The spatial vector map was derived from the National Catalogue Service for Geographic Information (http://www.webmap.cn).

As multicollinearity in the selected variables may cause information redundancy, we adopted the variance inflation factor (VIF) for multicollinearity diagnosis with a threshold of 5. We excluded the indicators of economic density and energy consumption because their VIF were greater than 5. Thus, 8 explanatory variables were used in the model including per capita GDP (*pgdp*), population density (*popd*), urbanization rate (*urba*), secondary industry share (*indu*), annual wind speed (*wind*), annual precipitation (*prec*), NDVI (*ndvi*), and topographic relief (*topo*). Furthermore, to reduce data fluctuation and heteroscedasticity, all the indicators were treated with Z–standardization.

Methods

Our empirical research frame is shown in Fig. 2. Firstly, we used the geographical vector data of the YREB to mask extract the aerosol optical depth (AOD) data retrieved from satellite data to estimate the spatial $PM_{2.5}$ concentration. Secondly, we investigated spatiotemporal differentiation of $PM_{2.5}$ pollution and its variation pattern via spatial autocorrelation and variogram analysis. Thirdly, we employed a geographically weighted regression and a novel statistical method, namely, geodetector models, to

quantitatively identify the individual and interactive impacts of natural and anthropogenic factors on urban $PM_{2.5}$ pollution.

Spatial autocorrelation analysis. Tobler's first law of geography states that "Everything is related to everything else. But near things are more related than distant things"[15]. Experience shows that $PM_{2.5}$ has both dependence and heterogeneity in space, and therefore, we adopted the classical spatial autocorrelation method to quantitatively measure the spatial dependence of $PM_{2.5}$ pollution in neighbouring regions. Global Moran's *I* is written as[36]:

$$I = \frac{n\sum_{i=1}^{n}\sum_{j=1}^{n} W_{ij}(x_i - \bar{x})(x_j - \bar{x})}{\sum_{i=1}^{n}\sum_{j=1}^{n} W_{ij}\sum_{i=1}^{n}(x_i - \bar{x})^2} \quad (1)$$

where x_i and x_j are the observations of spatial unit *i* and *j*, respectively; $\bar{x}$ is the mean of all observations at *n* locations; W_{ij} is a spatial weight matrix. The range of Moran's *I* is [−1, 1], $I > 0$ means positive correlation, $I < 0$ means negative correlation, and $I = 0$ means mutual independence.

Spatial variogram analysis. Spatial variogram, also called the semivariation function, is a geostatistical method to describe the structure and randomness of regionalized variables and is often used to effectively measure the spatial structure characteristics and variation law of geographical variables[37]. Our study introduces the spatial variogram to analyse the spatial variability law of $PM_{2.5}$ pollution. Variogram is expressed as:

$$\gamma(\lambda) = \frac{1}{2N(\lambda)}\sum_{i=1}^{N(\lambda)}[\xi(x_i) - \xi(x_i + \lambda)]^2 \quad (2)$$

where $\xi(x_i)$ and $\xi(x_i + \lambda)$ are the values of the regionalized variables at points x_i and $x_i + \lambda$, respectively, and $N(\lambda)$ is the sample size with a separation distance λ.

The variogram model can depict variations of $PM_{2.5}$ pollution in a graphical form, and a schematic diagram is presented in Fig. 3. The nugget parameter (C_0) is a random spatial variance; the partial sill parameter (C) is a structural spatial variance; the sill parameter (C_0+C) represents a total degree of spatial variation; and the nugget effect ($C_0/(C_0+C)$) indicates whether regional or local-scale factors are more important for $PM_{2.5}$ pollution distribution. If the nugget effect is less than 0.25, it indicates strong spatial correlation, if it is between 0.25 and 0.75, it shows moderate spatial correlation, and if it is greater than 0.75, it indicates weak spatial correlation. The range parameter (A_0) represents the maximum spatial

distance of $PM_{2.5}$ correlation. A variogram is usually fitted with spherical, linear, exponential, and Gaussian models.

Fractal dimension is another important parameter that characterizes the variogram and its value is determined by the relationship between the variogram $\gamma(\lambda)$ and distance λ:

$$2\gamma(\lambda) = \lambda^{(4-2D)} \quad (3)$$

where D is the slope of the double logarithm linear regression equation. The higher the value is, the higher is the heterogeneity caused by the spatial autocorrelation. The closer the value is to 2, the more balanced is the spatial distribution.

Geographically weighted regression modelling (*GWR*). GWR is a spatial regression model based on the idea of local smoothness[38]. This technique constructs an independent equation for each unit in the study area and incorporates the spatial attributes of data into the regression model so that the relationship between variables can change with the change of spatial location, thus reflecting the spatial non-stationarity of parameters in different regions. The GWR model structure is as follows:

$$y_i = \varphi_0(\omega_i, \alpha_i) + \sum_{i=1}^{p} \varphi_p(\omega_i, \alpha_i) x_{ip} + \varepsilon_i \quad (4)$$

where x_{ip} is a dimensional interpretation variable matrix; (ω_i, α_i) represents the longitude and latitude coordinates at the i^{th} observation point; $\varphi_p(\omega_i, \alpha_i)$ is the regression coefficient of the i^{th} observation point; and ε_i is a random error term.

Geographical detector technique. The geographical detector technique, originally proposed by Wang[39], is a set of statistical methods to detect spatially stratified heterogeneity and reveal the driving forces behind it. The geographical detector can detect the possible causal relationship between variables by verifying the consistency of the spatial distribution of two variables[40]. The factor explanatory power of the geodetector is measured by q value, and its expression is as follows:

$$q = 1 - \frac{\sum_{h=1}^{L} N_h \sigma_h^2}{N\sigma^2} \quad (5)$$

where L refers to the strata of variable Y ($PM_{2.5}$) or factor X; N_h and σ_h^2 are the number of units and variance of strata h, respectively; N and σ^2 are the total number of units and variance, respectively; and the value range of q is [0, 1], the greater the value is, the stronger is the explanatory power of the factor on $PM_{2.5}$ pollution.

The purpose of interactive detection is to assess whether the factors X_1 and X_2 work together to increase or decrease the explanatory power on Y ($PM_{2.5}$), or whether the impact of these factors on Y is independent. The evaluation method is to first calculate the q value of the two influencing factors X_1 and X_2 acting on Y: $q(X_1)$ and $q(X_2)$, and then calculate the q value for their interaction: $q(X_1 \cap X_2)$, and compare $q(X_1)$ and $q(X_2)$ with $q(X_1 \cap X_2)$. The criterion between the two factors can be divided into 5 categories (Table 1).

Results

Spatiotemporal evolutionary characteristics of $PM_{2.5}$. During 2000–2017, the overall $PM_{2.5}$ level in the YREB showed a trend of first increasing and then decreasing (Fig. 4a). During 2005–2010, the annual $PM_{2.5}$ concentration in the YREB was higher than the second-level standard of China of 35 μg/m^3. During 2000–2007, the $PM_{2.5}$ concentration increased from 23.49 μg/m^3 to 37.37 μg/m^3, an increase of 59.07%. Afterwards, it reduced to 31.79 μg/m^3 in 2017, a decrease of 14.93%. It is evident that 2007 was a turning point towards improvement in terms of $PM_{2.5}$. This improvement may be due to the effects of the national tenth five-year plan on controlling the total emission of major pollutants, adjusting industrial structure, and establishing a monitoring, statistics, and assessment system for energy conservation and pollution emission reduction. This was further reinforced by the implementation of the Action Plan for Air Pollution Prevention and Control in 2013 (http://www.mee.gov.cn).

Figure 4a shows that the sliding interval of the global Moran's I value over the years was [0.825, 0.894], and all the values were significant at the 99% level. This indicates that the $PM_{2.5}$ pollution distribution was not random, but it is a significant spatial agglomeration. We pursued the association of the evolution rules of spatial correlation with distance and found that the distance threshold to maintain spatial correlation was about 870 km (Fig. 4b). Within this spatial range, $PM_{2.5}$ had significant positive interaction effects, which increased with the shortening of distance. Beyond 870 km, the global correlation changed from positive to negative, and the $PM_{2.5}$ pollution among cities shifted from high–high clustering to low–high or high–low clustering.

Fig. 5 displays the spatial patterns and evolution of $PM_{2.5}$ pollution in the YREB from 2000 to 2017. Its main features are as follows: (1) Cities with annual $PM_{2.5}$ level of less than 15 μg/m^3 were mainly concentrated in ethnic minority areas, where the ecological and environmental conditions were relatively good. However, air quality was continuously deteriorating albeit at low levels, which needs attention. (2) In the Yangtze Basin the $PM_{2.5}$ level was higher in the lower reaches than the upper reaches and higher in the north bank than the south bank. The $PM_{2.5}$ level shows a diagonal spatial distribution pattern with an obvious lowland plain directivity. (3) Urban economic activities and population density were closely related to $PM_{2.5}$ pollution levels in three centres, namely, the Cheng-Yu economic zone of the upper reaches, the Wuhan metropolitan area of the middle reaches, and the northern Anhui–Jiangsu region of the lower reaches[41].

Spatiotemporal variation characteristics of $PM_{2.5}$. We further explored the spatial heterogeneity evolution of $PM_{2.5}$ pollution in the YREB by using the variogram geostatistical method (Table 2). The value of the variogram increased with the increase in separation distance indicating that the spatial autocorrelation of $PM_{2.5}$ pollution changed from strong to weak with the increase of distance. During 2000–2017, the variation range of $PM_{2.5}$ pollution was 625–738 km, and it showed an overall upward trend implying that the spatial correlation of $PM_{2.5}$ pollution was partly expanded in scope. The higher the sill parameter is, the higher is the spatial heterogeneity. Therefore, the spatial heterogeneity of $PM_{2.5}$ pollution was the lowest in 2017. In addition, the nugget effect indicated that regional scale influencing factors are more important for the distribution of $PM_{2.5}$ pollution.

In terms of the fractal dimension (Table 3), the isotropic dimension continuously decreased from 1.536 in 2000 to 1.453 in 2017 indicating that the spatial difference of $PM_{2.5}$ pollution was continuously expanding. The northeast–southwest direction had the greatest goodness of fit, the smallest fractal dimension, and showed a downward trend. This denoted that the spatial variation of $PM_{2.5}$ pollution in this direction was continuously strengthened making it the main direction in terms of spatial difference. The southeast–northwest fractal dimension was the largest and its decisive coefficient kept decreasing showing that the spatial difference of $PM_{2.5}$ pollution in this direction continued to weaken and remained relatively evenly balanced. The south–north fractal dimension first rose and then fell suggesting that the variability of the spatial pattern of $PM_{2.5}$ pollution in this direction was enhanced. The change in the east–west fractal dimension indicated spatial heterogeneity of $PM_{2.5}$ pollution in this direction and the degree of differentiation kept increasing with time. We conducted 3D-kriging interpolation, which further depicted the spatial distribution and evolution morphology of $PM_{2.5}$ pollution (Fig. 6). It was evident that the overall $PM_{2.5}$ level showed a distribution pattern with a higher value in the east and lower value in the west. Furthermore, $PM_{2.5}$ pollution pattern was steadily transitioned from a gradient differentiation to a relatively balanced structure that formed a trend indicating that the middle–lower reaches of the Yangtze drove the whole basin $PM_{2.5}$ level to increase.

Influence factor analysis models

GWR model results. GWR model fitting results are shown in Table 4, in which the adjusted R^2 values were above 0.9 indicating a good fitting performance.

The regression coefficients of socioeconomic factors such as per capita GDP, population density, urbanization rate, and industrial structure were mainly positive. Among them, population density had the largest impact on $PM_{2.5}$ and the most obvious spatial difference, followed by per capita GDP, while the coefficients of urbanization and industrial structure were relatively small. The regression coefficients of natural environmental factors such as wind, precipitation, vegetation, and topography were distributed in positive and negative intervals, and the instability was striking in different years. Among them, the coefficient of distribution interval for topographic relief was the longest indicating that spatial

heterogeneity was the largest. While the coefficient of distribution interval for NDVI was shorter showing that the spatial heterogeneity was small.

Spatial heterogeneity of influencing factors. During 2000–2007, overall, the coefficient of socioeconomic factors increased signifying that extensive economic development and intensive human activities aggravated $PM_{2.5}$ pollution. During this period, the coefficient declined but did not turn negative implying that the effects of economic development on environmental improvement did not appear yet. Existing studies have argued that economic development strongly correlates with regional haze pollution, in particular, the relationship between per capita GDP and $PM_{2.5}$ level was significantly different in various regions[19]. Per capita GDP had positive impacts on $PM_{2.5}$ in the middle–upper reaches of the Yangtze Basin (Fig. 7a, b, c). This implied that $PM_{2.5}$ pollution in economically backward areas was more sensitive to economic development and economic growth of these regions came at the cost of the environment. Some cities in the YRD show negative correlation effects, which indicate that the development planning in the above areas was relatively good. With technological progress and industrial upgradation, economic development of these areas are essentially in coordination with the surroundings.

The coefficient of population density showed approximately the same spatial distribution at the three time nodes (Fig. 7d, e, f), all of which increased from the coastal areas to the inland areas, and among them the east–west difference was obvious in 2017. This may be because of the increase in urban traffic flow and production with a higher population density contributing to an increase in the local $PM_{2.5}$ level. The control of air pollution in the middle–upper reaches of the Yangtze Basin was still weak, thereby, making the impact of population density more significant. Some studies have held that the increase of population density may have an agglomeration effect in promoting regional technical progress, and thus, facilitating the reduction of the local $PM_{2.5}$ level[14]. The technical advances brought by the agglomeration effect for the population size in the YREB was not significant. This may be related to the migration of people to big cities in the recent years and the disordered nature of population mobility.

The coefficient of urbanization rate was positive at the three time nodes. The proportion of positive values in 2007 was relatively large, and the positive values in 2017 has marginally declined (Fig. 7g, h, i). During 2000–2007, areas with low urbanization rate in the Yangtze Basin were experiencing rapid urbanization and the urban infrastructure industry developed rapidly[9]. A large quantity of building dust entered the atmosphere aggravating urban $PM_{2.5}$ pollution. However, areas with high urbanization rate, such as the YRD, tend to mature and a stagnant infrastructure industry is conducive for reduction in emission of fine particles.

The industrial structure had a negative impact on $PM_{2.5}$ level in the middle–lower Yangtze plains and the Sichuan–Chongqing areas (Fig. 7j, k, l) aggravating local air pollution. This is consistent with findings of existing studies confirming that industrial activities were the main drivers of $PM_{2.5}$ pollution in most areas[19]. The impact of the industrial structure in Sichuan–Chongqing areas was strong, which may be because of heavy industries such as energy, chemical, and machinery with relatively high direct energy

consumption and pollutant emission. The optimization and adjustment of the industrial structure will significantly affect the local $PM_{2.5}$ level in the air. The coefficient had a weak impact on $PM_{2.5}$ in the YRD area, because the local industrial structure was dominated by the service industry and it was relatively stable, and thus, there was limited scope for further optimization.

The impact of intensity of wind speed on regional $PM_{2.5}$ showed obvious east–west differences. The coefficients in the central and western areas were mainly positive and decreased from the central region to the west (Fig. 7m, n, o). The negative impact was dominant in the eastern areas, and as the distance to the coast reduced, the negative impact increased. This may be related to the impacts of topography and monsoon. Coastal areas were mostly alluvial plains with flat terrains, and they were affected by the local circulation caused by monsoon and temperature differences[27]. Clean air from the ocean had important dilution effects on pollutants, and thus, the coefficient was mainly negative. In the central and western areas, especially in the Sichuan Basin, the impact of closed topography restricted the diffusion of airflow and the transport of wind caused pollutants in the region to interact with each other, and thus, the coefficient was mainly positive. Similar findings were made in the Fenwei Plain, where a basin topography exists[30].

The impact of precipitation on regional $PM_{2.5}$ concentration presented a negative correlation at the three time nodes (Fig. 7p, q, r). A positive influence was mainly distributed in the Sichuan Basin and some areas of the Yunnan–Guizhou Plateau in western China, while the negative effect decreased from the coastal areas to inland areas. In terms of spatial heterogeneity, the regions with a high regression coefficient were mainly located in the upper and middle reaches of the Yangtze Basin, while the eastern coastal areas with abundant rainfall had a small regression coefficient indicating that abundant precipitation had a positive impact on $PM_{2.5}$ pollution in most cities, and this effect was more distinct in areas with relatively deficient precipitation.

The impact of NDVI on regional $PM_{2.5}$ concentration had a negative correlation that was mainly distributed in the middle–lower Yangtze plains (Fig. 7s, t, u). Research has shown that vegetation growth is correlated with climate and is affected by topography and human activities resulting in a complex correlation between vegetation and $PM_{2.5}$[21]. The spatial distribution of coefficients shows that the high-value areas were mainly in Yunnan,and Hunan provinces, while the low-value areas were concentrated in the middle–lower Yangtze plain areas. In 2017, the NDVI showed a negative impact indicating vegetation's inhibitory effect on $PM_{2.5}$ pollution was distinctly enhanced. This may be related to the rapid restoration and development of vegetation in the Yangtze Basin whose forest coverage rate has risen from 24% in 2000 to 39% in 2017[9]. Thus, vegetation is an important inhibiting factor for $PM_{2.5}$.

Topographic relief was negatively correlated with regional $PM_{2.5}$ pollution in the Yangtze Basin, which was conducive to the improvement in air quality. From the spatial distribution of the coefficient (Fig. 7v, w, x), the high-value regions were located in Sichuan, Chongqing, and Zhejiang. The lower values were

concentrated in the middle–lower reaches of the Yangtze. Local topography affects the diffusion and dilution of atmospheric pollutants in an area by influencing meteorological conditions[20].

Interactions of influencing factors. Table 5 shows the results of the interactions of the influencing factors. The impact of the interactions between factors was greater than that of individual factors, and the interaction types included nonlinear enhancement and bi-factor enhancement. In terms of socioeconomic factors, when industrial structure interacted with per capita GDP and urbanization level on urban $PM_{2.5}$ pollution, a nonlinear enhancement effect was exerted at all three time nodes, and the explanatory power was continuously improved. When annual average wind speed, annual precipitation, and vegetation coverage (natural factors) interacted with urban $PM_{2.5}$ level in pairs, the nonlinear enhancement effect was generated at all three time nodes, and the explanatory power was notably varied in different periods. Nonlinear enhancement means that the interactive impact of two factors is greater than the sum of the impacts when they act alone. The interactive types of *pgdp* ∩ *popd*, *pgdp* ∩ *urba*, *wind* ∩ *topo*, *prec* ∩ *topo*, and *ndvi* ∩ *topo* were dominated by nonlinear enhancement though they were varied in different years. The interactive types of *popd* ∩ *urba* and *popd* ∩ *indu* exerted a bi-factor enhancement effect, which was not as significant as that of the nonlinear enhancement.

Conclusions And Policy Implications

Conclusions. $PM_{2.5}$ pollution in Chinese cities has escalated to hazardous levels in recent years. This environmental problem has become a great challenge for public health and urban sustainable development. Our exploration of $PM_{2.5}$ pollution in the YREB provides useful results for haze prediction, which is an important step toward protecting people from health damages caused by poor air quality. The results indicate that the annual $PM_{2.5}$ level of the YREB displayed an upward trend prior to 2007 and a fluctuating downward trend after that, and then, it gradually stabilized. $PM_{2.5}$ pollution in the Yangtze Basin has significant spatial heterogeneity and convergence characteristics. The spatial variability of $PM_{2.5}$ pollution has been enlarged and its main fractal dimension was established as trending in the northeast–southwest direction. There were clear spatiotemporal differences in the impact of various factors on $PM_{2.5}$ pollution pattern. In the socioeconomic layer, population density has the greatest impact, followed by per capita GDP and secondary industry share, while urbanization was a relatively stable factor causing the rise of $PM_{2.5}$ level. Among the natural factors, topography and vegetation mainly exerted a negative impact on $PM_{2.5}$ pollution, while the potency and direction of others changed with the change of time and space. The impact of interaction between factors was greater than that of single factors, and the interactive types included nonlinear and bi-factor enhancements.

Policy implications. As the Yangtze River plays a vital role in China's ecological and environmental systems, some stricter measures should be implemented to meet the goal of sustainable development. Firstly, to efficiently alleviate and control $PM_{2.5}$ pollution, special attention should be paid to natural factors when distributing industries and residences, for instance, topography and wind, which notably affect $PM_{2.5}$ level should be considered. In addition, urban air duct and green belt design must be

optimized. Secondly, given that natural and socioeconomic conditions vary region wise in the YREB, region-targeted policies should be considered based on spatial differentiation. Downstream areas should play a leading role in promoting pollution prevention and control technologies, while upstream areas should actively drive ecological protection. More emphasis should be placed on transregional linkage governance when formulating mitigation measures for $PM_{2.5}$ pollution. Thirdly, heavy and highly polluted industrial sectors must be closed or upgraded as they are major sources of $PM_{2.5}$ pollution, while sectors with environmental protection, new energy, and low-carbon economy and technology should be highly encouraged. Local governments should build hi-tech eco-industrial parks and advance industrial upgradation to improve air quality without hindering local economic growth. Lastly, it seems inevitable that air pollution will aggravate because of the burgeoning urbanization, and therefore, reducing the impact of anthropogenic activity on the atmosphere through environmental publicity and education will reduce $PM_{2.5}$ pollution.

Declarations

Acknowledgements

This study was funded by the National Key Research and Development Program of China (No. 2016YFA0602800), The Strategic Priority Research Program of the CAS, (No. XDA20040400), National Natural Science Foundation of China (No. 41871118, No. 41271141) and Young Scientist Project of Institute of Geographic Sciences and Natural Resources Research, CAS (No.2016RC202)

Author Contributions

All authors contributed to the study conception and design. Siyou Xia: Methodology, Writing- Original draft preparation; Yu Yang: Conceptualization, Reviewing, Editing and Project administration; Xiaojie Liu: Writing- Original draft preparation, Methodology, Formal analysis; Qing Liu: Data analysis, Investigation; Yannan Zhou: Visualization, Data analysis.

Competing interests

The authors declare that they have no conflict of interest.

References

1. Lelieveld, J., Evans, J. S. & Fnais, M. The contribution of outdoor air pollution sources to premature mortality on a global scale. *Nature*, **525** (7569), 367–371 (2015).
2. Kan, H. D., Chen, R. J. & Tong, S. L. Ambient air pollution, climate change, and population health in China. *Environ Int*, **42** (7), 10–19 (2012).
3. Figueres, C. & Landrigan, P. J. Tackling air pollution, climate change, and NCDs: time to pull together., **392**, 1502–1503 (2018).

4. Jin, Y., Andersson, H. & Zhang, S. Air pollution control policies in China: a retrospective and prospects. *Int. J. Environ. Res. Public Health*, **13** (12), 1219 (2016).
5. Samet, J. M., Dominici, F. & Curriero, F. C. Fine particulate air pollution and mortality in 20 U.S. cities, 1987–1994. *N. Engl. J. Med*, **343** (24), 1742–1749 (2000).
6. Yin, P., Michael, B., Aaron, J. C. & Wang, H. D. The effect of air pollution on deaths, disease burden, and life expectancy across China and its provinces, 1990–2017: an analysis for the Global Burden of Disease Study 2017. Lancet Planet Health. DOI: https://doi.org/10.1016/S2542-5196(20)30161-3(2020).
7. Xu, P., Chen, Y. F. & Ye, X. J. Haze, air pollution, and health in China., **382** (9910), 2067–2067 (2013).
8. Tian, X., Dai, H., Geng, Y., Wilson, J. & Wu, R. Economic impacts from PM2.5 pollution–related health effects in China's road transport sector: a provincial–level analysis. *Environ. Int*, **115**, 220–229 (2018).
9. Chen, Y. S., Zhang, S. H. & Huang, D. S. The development of China's Yangtze River Economic Belt: how to make it in a green way? *Sci. Bull*, **62**, 1–20 (2017).
10. Li, M. N. & Zhang, L. L. Haze in China: Current and future challenges. *Environ. Pollut*, **189**, 85–86 (2014).
11. Ye, W. F., Ma, Z. Y. & Ha, X. Z. Spatial–temporal patterns of PM2.5 concentrations for 338 Chinese cities. *Sci. Total Environ*, **631–632**, 524–533 (2018).
12. Ma, Z. *et al.* Satellite–based spatiotemporal trends in PM2.5 concentrations: China, 2004–2013. *Environ. Health Perspect*, **124**, 184–192 (2016).
13. Wang, S. J., Zhou, C. S. & Wang, Z. B. The characteristics and drivers of fine particulate matter (PM2.5) distribution in China. *J. Clean. Prod*, **142**, 1800–1809 (2017).
14. Zhou, C. J., Chen, J. & Wang, S. J. Examining the effects of socioeconomic development on fine particulate matter (PM2.5) in China's cities using spatial regression and the geographical detector technique. *Sci. Total Environ*, **619–620**, 436–445 (2018).
15. Tobler, W. R. A computer movie simulation urban growth in the Detroit region. *Econ. Geogr*, **46**, 234–240 (1970).
16. Wang, Z. & Fang, C. Spatial–temporal characteristics and determinants of PM2.5 in the Bohai Rim urban agglomeration. *Chemosphere*, **148**, 148–162 (2016).
17. Zhang, Y. & Cao, F. Fine particulate matter (PM2.5) in China at a city level. *Sci. Rep*, **5**, 14884 (2015).
18. Huang, R. J. *et al.* High secondary aerosol contribution to particulate pollution during haze events in China. *Nature*, **514**, 218–222 (2014).
19. Liu, H. *et al.* The effect of natural and anthropogenic factors on haze pollution in Chinese cities: a spatial econometrics approach. *J. Clean. Prod*, **165**, 323–333 (2017).
20. Alvarez, H. B., Echeverria, R. S., Alvarez, P. S. & Krupa, S. Air quality standards for particulate matter (pm) at high altitude cities. *Environ. Pollut*, **173**, 255–256 (2013).

21. Wang, S. J., Liu, X. P. & Yang Spatial variations of PM2.5 in Chinese cities for the joint impacts of human activities and natural conditions: A global and local regression perspective. *J. Clean. Prod*, **203**, 143–152 (2018).
22. Guan, D. *et al.* The socioeconomic drivers of China's primary PM2.5 emissions. *Environ. Res. Lett*, **9**, 024010 (2014).
23. Xu, X., Gonzalez, J. E., Shen, S., Miao, S. & Dou, J. Impacts of urbanization and air pollution on building energy demands–beijing case study. *Appl. Energy*, **225**, 98–109 (2018).
24. Xu, S. C., Miao, Y. M., Gao, C. & Long, R. Y. Regional differences in impacts of economic growth and urbanization on air pollutants in China based on provincial panel estimation. *J. Clean. Prod*, **208**, 340–352 (2019).
25. Lu, D. D. Conservation of the Yangtza River and sustainable development of the Yangtze River Economic Belt:An understanding of General Secretary Xi Jinping's important instructions and suggestions for their implementation. *Acta Geogr Sin*, **73** (10), 1829–1836 (2018).
26. Zhong, Y., Lin, A., He, L. J., Zhou, Z. G. & Yuan, M. X. Spatiotemporal dynamics and driving forces of urban land–use expansion: a case study of the Yangtze River Economic Belt, China. *Rem. Sens*, **12** (2), 287 (2020).
27. Yang, M. & Wang, Y. Spatial–temporal characteristics of PM2.5 and its influencing factors in the Yangtze River economic Belt. *China Popul. Resour. Environ*, **27**, 91–100 (2017).
28. Zhu, W. W., Wang, M. C. & Zhang, B. B. The effects of urbanization on PM2.5 concentrations in China's Yangtze River Economic Belt: new evidence from spatial econometric analysis. *J. Clean. Prod*, **239**, 1–10 (2019).
29. Feng, Y. Y. *et al.* Defending blue sky in China: Effectiveness of the "Air Pollution Prevention and Control Action Plan" on air quality improvements from 2013 to 2017. *J. Environ. Manage*, **252**, 109603 (2019).
30. Zhou, L. *et al.* Spatio–temporal evolution and the influencing factors of PM2.5 in China between 2000 and 2015. *J. Geogr. Sci*, **29** (2), 253–270 (2019).
31. Guo, J., Zhu, D., Wu, X. & Yan, Y. Study on environment performance evaluation and regional differences of strictly–environmental–monitored cities in China. *Sustainability*, **9**, 2094 (2017).
32. Cheng, Z., Li, L. & Liu, J. Identifying the spatial effects and driving factors of urban PM2.5 pollution in China. *Ecol. Indicat*, **82**, 61–75 (2017).
33. Wu, W. Q., Zhang, M. & Ding, Y. T. Exploring the effect of economic and environment factors on PM2.5 concentration: A case study of the Beijing-Tianjin-Hebei region. *J. Environ. Manage*, **268**, 110703 (2020).
34. Van, D. A., Martin, R. V. & Brauer, M. Global estimates of fine particulate matter using a combined geophysical statistical method with information from satellites, models, and monitors. *Environ. Sci. Technol*, **50** (7), 3762–3772 (2016).
35. Xie, Y. Weng. Q. World energy consumption pattern as revealed by DMSP–OLS nighttime light imagery. *GISCI REMOTE SENS*, **53** (2), 265–282 (2016).

36. Moran, P. Notes on Continuous Stochastic Phenomena. *Biometrika*, **37**, 17–23 (1950).
37. Song, W. Z., Jia, H. F., Li, Z. L. & Tang, D. L. Using geographical semi–variogram method to quantify the difference between NO2 and PM2.5 spatial distribution characteristics in urban areas. *Sci. Total Environ*, **631–632**, 688–694 (2018).
38. Fotheringham, A. S. & Brunsdon, C. Local forms of spatial analysis. *Geogr Anal*, **31** (4), 340–358 (1999).
39. Wang, J. F., Li, X. H. & Christakos, G. Geographical detectors–based health risk assessment and its application in the neural tube defects study of the Heshun region, China. *Int. J. Geogr. Inf. Sci*, **24** (1), 107–127 (2010).
40. Wang, J. F. & Xu, C. D. Geodetector: principle and prospective. *Acta Geograplica Sin*, **1**, 116–134 (2017).
41. Liu, X. J., Xia, S. Y. & Yang, Y. Spatiotemporal dynamics and impacts of socioeconomic and natural conditions on PM2.5 in the Yangtze River Economic Belt. *Environ. Pollut*, **263**, 114569 (2020).

Tables

Table 1. Types of interaction between two covariates

Diagram	Criterion	Interaction
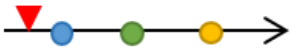	$q(X_1 \cap X_2) < \text{Min}(q(X_1), q(X_2))$	Nonlinear weakening
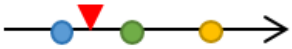	$\text{Min}(q(X_1), q(X_2)) < q(X_1 \cap X_2) < \text{Max}(q(X_1), q(X_2))$	Univariate nonlinear weakening
	$q(X_1 \cap X_2) > \text{Max}(q(X_1), q(X_2))$	Bivariate enhancement
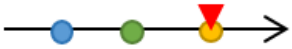	$q(X_1 \cap X_2) = q(X_1) + q(X_2)$	Independent
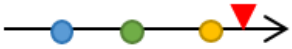	$q(X_1 \cap X_2) > q(X_1) + q(X_2)$	Nonlinear enhancement

Note: Min($q(X_1)$, $q(X_2)$) is the minimum value between $q(X_1)$ and $q(X_2)$; Max($q(X_1)$, $q(X_2)$) is the maximum value between $q(X_1)$ and $q(X_2)$; $q(X_1)+q(X_2)$ is the sum of $q(X_1)$ and $q(X_2)$; $q(X_1 \cap X_2)$ is the interaction between $q(X_1)$ and $q(X_2)$.

Table 2
Fitting parameters of $PM_{2.5}$ concentration variogram

Year	A_0 (km)	C_0	C_0+C	$C_0/(C_0+C)$	R^2	Residual sum of squares	Optimal fitting model
2000	625.27	0.0029	0.0543	0.0534	0.960	2.061E-04	Gaussian
2007	737.85	0.0036	0.0492	0.0732	0.963	1.444E-04	Gaussian
2017	635.66	0.0011	0.0484	0.0227	0.987	5.271E-05	Gaussian

Table 3
Variable difference dimension of $PM_{2.5}$ concentration

Year	Isotropic		South–North (0°)		Northeast–Southwest (45°)		East–West (90°)		Southeast–Northwest (135°)	
	D	R^2	D	R^2	D	R^2	D	R^2	D	R^2
2000	1.536	0.959	1.517	0.847	1.430	0.985	1.603	0.918	1.527	0.922
2007	1.482	0.977	1.554	0.763	1.409	0.997	1.464	0.914	1.520	0.756
2017	1.453	0.936	1.509	0.774	1.292	0.985	1.258	0.787	1.567	0.611

Table 4
Fitting results of GWR model

Variables and parameters	2000	2007	2017
pgdp	-0.2792–0.4534*	-0.1764–0.6815**	-0.1982–0.4392*
popd	-0.2327–1.2928**	0.0070–0.9061***	-0.0448–1.4807***
urba	-0.2099–0.5177**	-0.0996–0.3314*	-0.1814–0.1884**
indu	-0.1569–0.1629*	-0.1711–0.2928*	-0.0612–0.1158***
wind	-1.5755–0.2788***	-0.6810–0.1470***	-0.4908–0.3147*
prec	-0.8223–0.4898***	-0.3110–0.0518*	-0.2301–0.3349**
ndvi	-0.6251–0.0474***	-0.7815–0.0027***	-0.5942– -0.0026**
topo	-0.6420–0.1005***	-0.7488– -0.1018***	-1.1785– -0.1100***
Bandwidth	3.321	3.627	3.289
AICc	118.931	51.926	16.542
R^2	0.949	0.966	0.977
Adjusted R^2	0.913	0.944	0.960
Note: *, ** and *** indicate significance at the 10%, 5% and 1% level, respectively.			

Table 5
Results of interaction detecting

Factors	2000	2007	2017	Factors	2000	2007	2017
pgdp ∩ popd	NE(0.682)	NE(0.745)	BE(0.709)	wind ∩ prec	NE(0.624)	NE(0.488)	NE(0.749)
pgdp ∩ urba	NE(0.281)	NE(0.420)	BE(0.421)	wind ∩ ndvi	NE(0.570)	NE(0.486)	0.814(NE)
pgdp ∩ indu	NE(0.370)	NE(0.225)	NE(0.472)	wind ∩ topo	NE(0.666)	NE(0.794)	BE(0.843)
popd ∩ urba	NE(0.654)	BE(0.757)	BE(0.748)	prec ∩ ndvi	NE(0.442)	NE(0.427)	NE(0.373)
popd ∩ indu	BE(0.657)	NE(0.747)	BE(0.762)	prec ∩ topo	NE(0.602)	BE(0.757)	NE(0.841)
urba ∩ indu	NE(0.397)	NE(0.432)	NE(0.516)	ndvi ∩ topo	NE(0.649)	NE(0.842)	BE(0.847)
Note: NE represents a nonlinear enhancement, BE represents a bi-factor enhancement.							

Figures

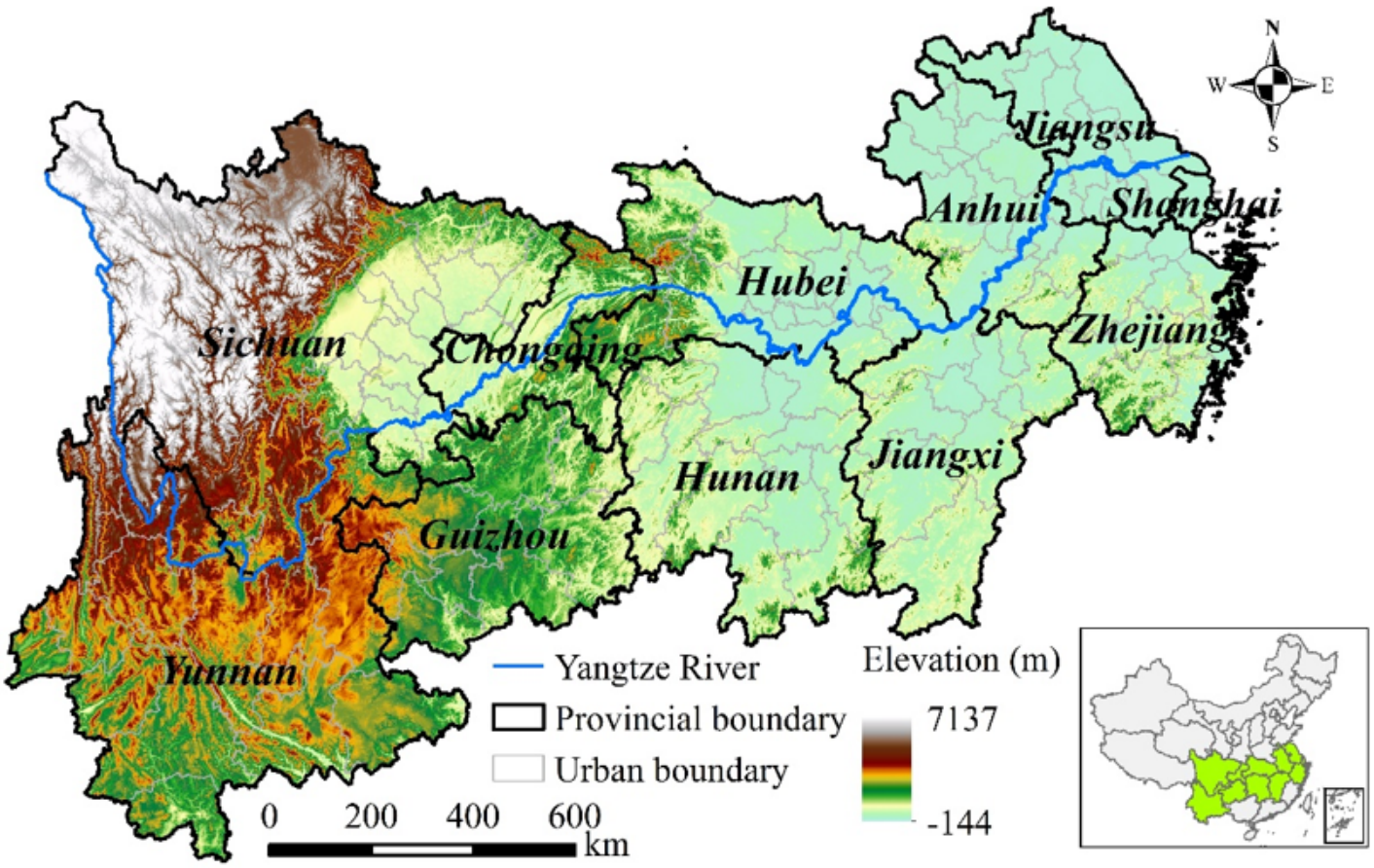

Figure 1

A general overview of the YREB

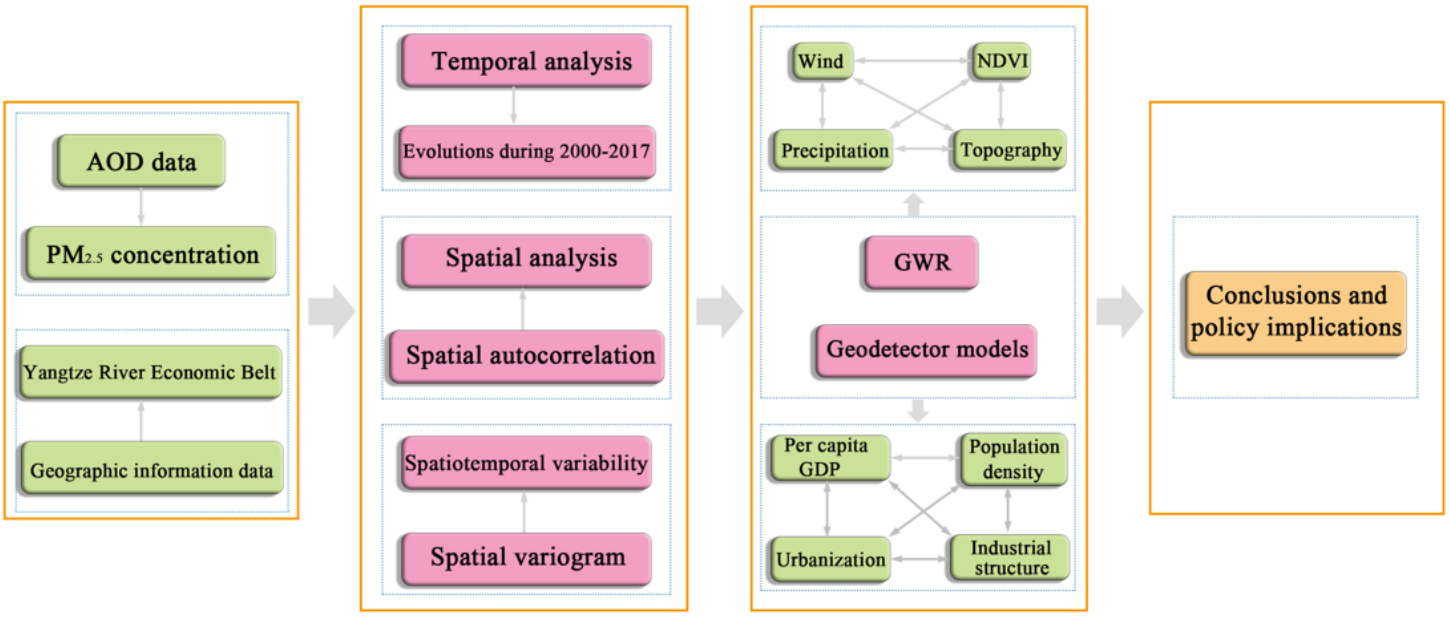

Figure 2

Flowchart of the methodology

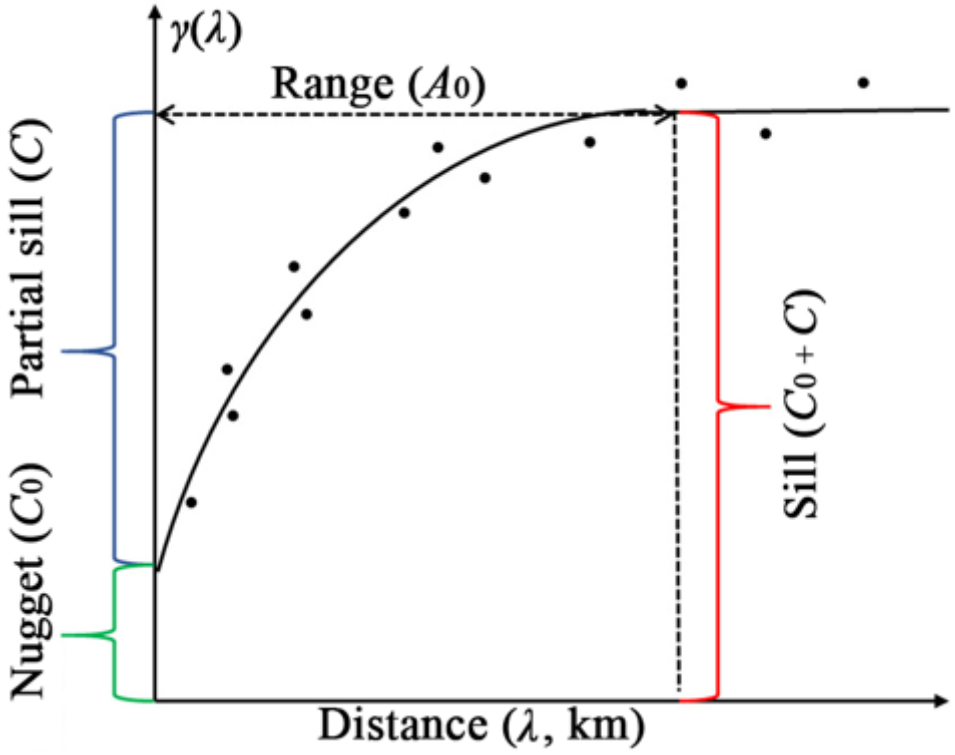

Figure 3

Schematic diagram of the variogram analysis

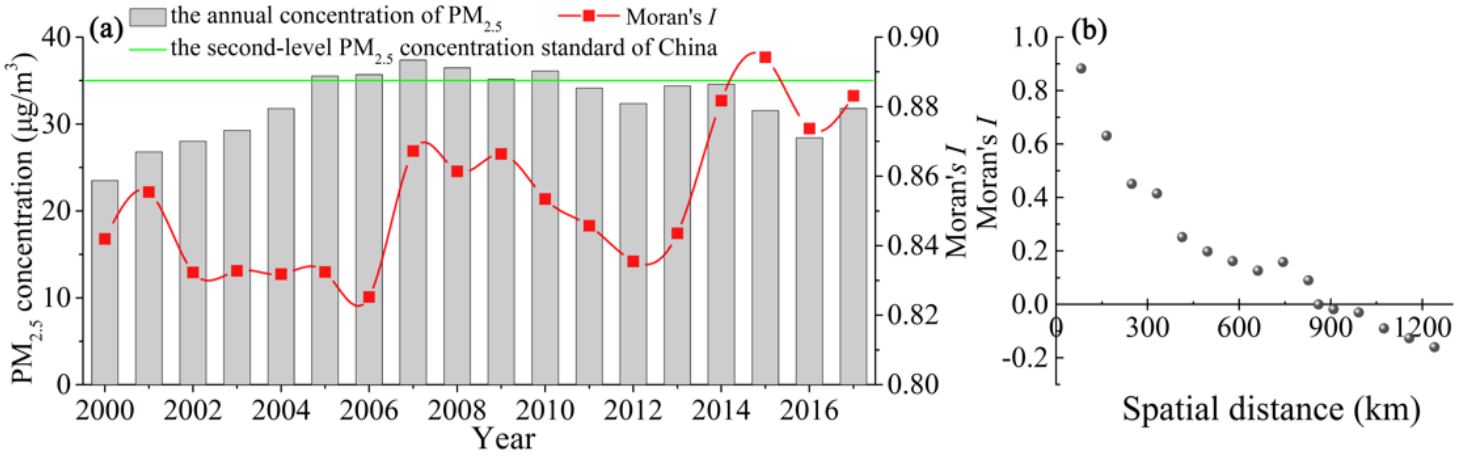

Figure 4

Variation trend of PM2.5 concentration and Moran's I value in the YREB

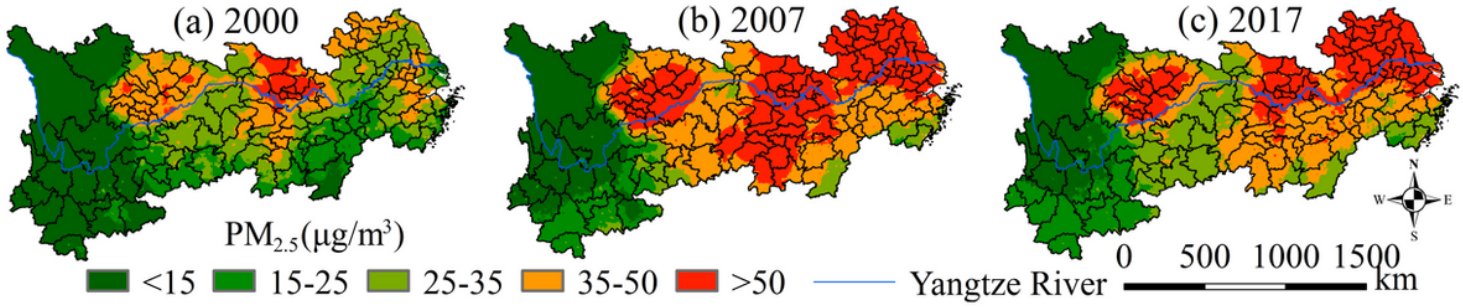

Figure 5

Spatial patterns of PM2.5 pollution in the YREB between 2000 and 2017

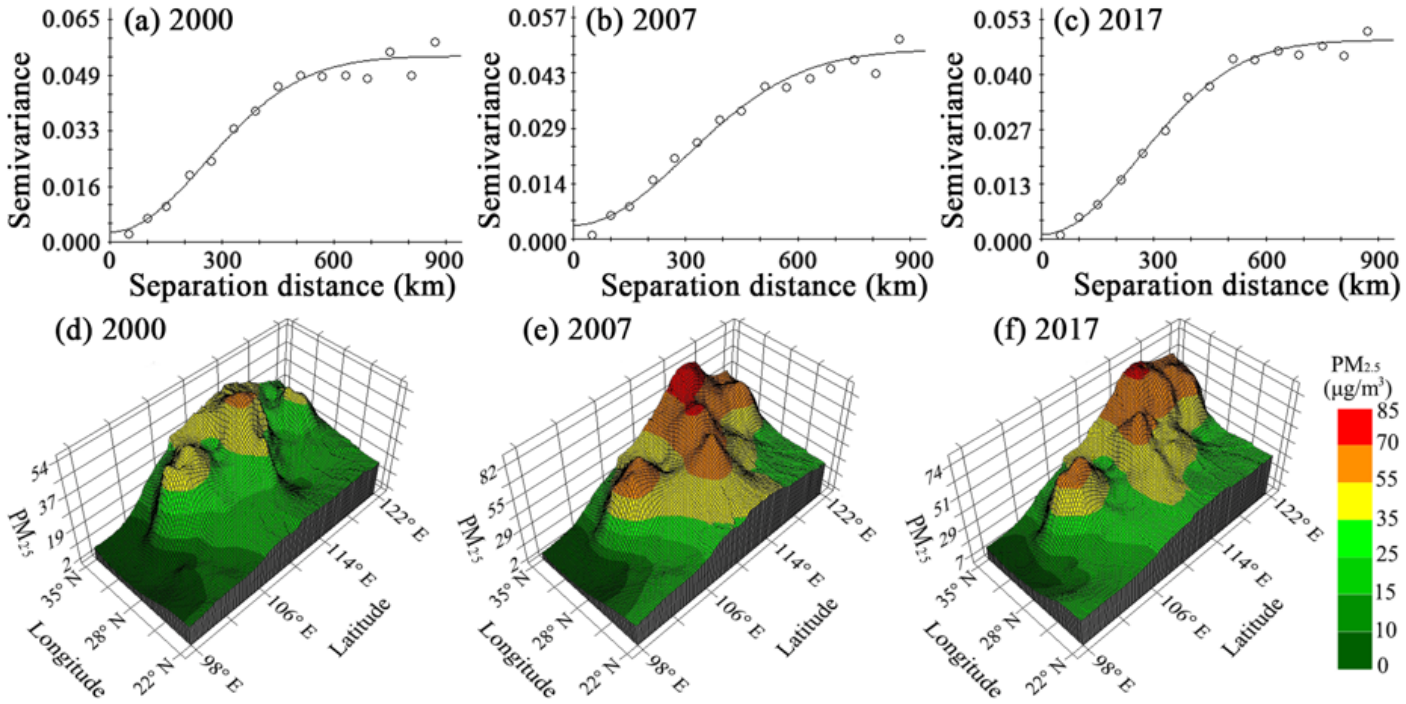

Figure 6

Evolution of PM2.5 concentration in the YREB based on variograms

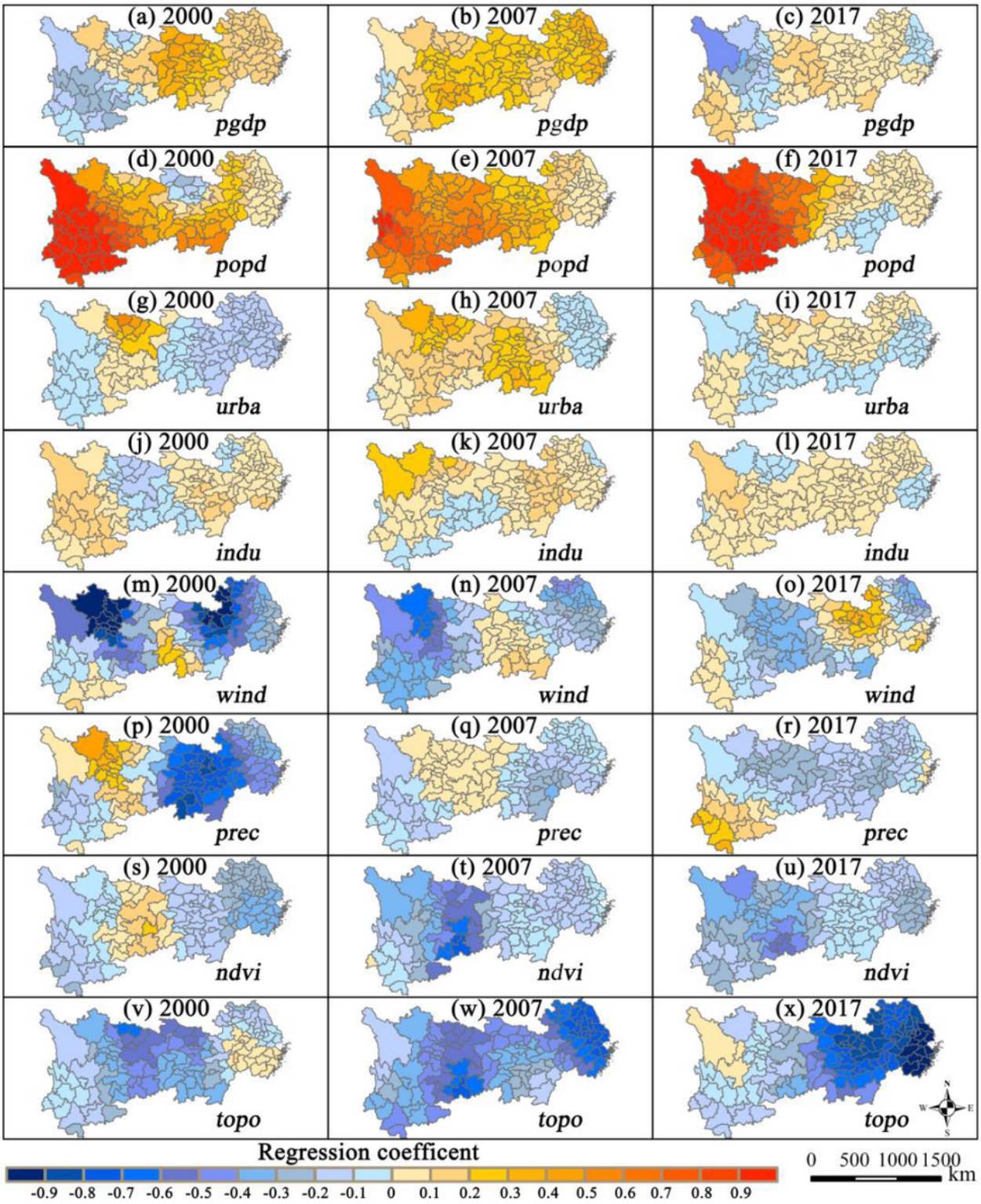

Figure 7

Spatial distribution of regression coefficients of the GWR model